

Low-Molecular Weight and Oligomeric Components in Secondary Organic Aerosol from the Photooxidation of p-Xylene

Ming-Qiang Huang* (黃明強), Wei-Jun Zhang (張為俊), Li-Qing Hao (郝立慶),
Zhen-Ya Wang (王振亞), Wen-Wu Zhao (趙文武),
Xue-Jun Gu (顧學軍) and Li Fang (方黎)
*Laboratory of Environment Spectroscopy, Anhui Institute of Optics & Fine Mechanics,
Chinese Academy of Sciences, Hefei 230031, P. R. China*

A laboratory study was performed to investigate the composition of secondary organic aerosol (SOA) products from photooxidation of the aromatic hydrocarbon p-xylene. The experiments were conducted by irradiating p-xylene/CH₃ONO/NO/air mixtures in a home-made smog chamber. The aerosol time-of-flight mass spectrometer (ATOFMS) was used to measure the size and the chemical composition of individual secondary organic aerosol particles in real-time. According to a large number of single aerosol diameters and mass spectra, the size distribution and chemical composition of SOA were determined statistically. Experimental results showed that aerosol created by p-xylene photooxidation is predominantly in the form of fine particles, which have diameters less than 2.5 μm (i.e. PM_{2.5}), and aromatic aldehyde, unsaturated dicarbonyls, hydroxyl dicarbonyls, and organic acid are major product components in the SOA after 2 hours photooxidation. After aging for more than 8 hours, about 10% of the particle mass consists of oligomers with a molecular mass up to 600 daltons. The possible reaction mechanisms leading to these products are also proposed.

Keywords: p-Xylene; Secondary organic aerosol; Oligomers; Smog chamber; Laser desorption/ionization; Reaction mechanisms.

INTRODUCTION

It is well known that aromatic compounds such as benzene, toluene, ethylbenzene, and xylenes (BTEX) are important constituents of automobile tailpipe exhaust and evaporative emissions.¹⁻⁴ In addition to their important role in photochemical ozone production, oxidation of aromatic compounds leads to formation of nonvolatile and semi-volatile organic compounds, which are responsible for secondary organic aerosol (SOA) in urban air.⁵ Recently, evidence has been found for the formation of oligomers from photooxidation of aromatic hydrocarbons.^{6,7} The existence of oligomers in SOA has significant implications for the physical behavior of the SOA particles in the atmosphere, as well as for their behavior in atmospheric models.

p-Xylene is an important constituent of aromatic hydrocarbons and is highly reactive with respect to ozone formation. In the atmosphere, the dominant loss process for p-xylene is the gas-phase reaction with the hydroxyl radical OH. Its reaction rate with OH radicals is on the order of 10⁻¹¹ cm³ molecule⁻¹ s⁻¹, nearly four times higher than that

of toluene.⁸ The OH-initiated reaction results in minor H-abstraction from one methyl group to form a methylbenzyl radical (about 10%) and major OH addition to the aromatic ring to form a dimethylhydroxycyclohexadienyl radical (about 90%).⁹ As shown in Fig. 1, in the presence of O₂ and NO, the subsequent reactions of the methylbenzyl radical lead to the formation of p-tolualdehyde. Under atmospheric conditions, the dimethylhydroxycyclohexadienyl radical (the OH-p-xylene adduct) reacts with O₂ either by O₂ addition to form primary peroxy radicals or by H-abstraction to yield 2,5-dimethylphenol, or by H-abstraction to form aromatic oxide/oxepin. The fate of the primary peroxy radicals is governed by competition between reaction with NO to form alkoxy radicals and intramolecular cyclization to form bicyclic radicals. Theoretical studies have shown that, instead of reaction with NO, the primary peroxy radicals from the OH-initiated oxidation of toluene cyclize, forming bicyclic radicals.¹⁰ In the presence of NO, subsequent reactions of bicyclic radicals resulting from the OH-initiated of the p-xylene lead to multi-functional or-

* Corresponding author. E-mail: huangmingqiang@gmail.com

ganic compounds such as glyoxal, methylglyoxal, and unsaturated carbonyl compounds. The aromatic oxide/oxepin channel lead to the formation of unsaturated dicarbonyls, although it remains uncertain.

Numerous experiments have been carried out to study the products from OH-initiated p-xylene oxidation,¹¹⁻¹⁷ and chemical composition of p-xylene SOA particle formed in chambers have been studied using off-line techniques, which have provided important information about the chemical compositions. However, the off-line techniques are time-consuming and tend to have sampling artifacts.¹⁸ In addition, it is difficult to measure the size and chemical compositions of the individual SOA particles simultaneously and in real-time by using the off-line techniques. We have demonstrated that aerosol time-of-flight mass spectrometer (ATOFMS) can be used to measure the size and chemical composition of toluene SOA particles in real-time.¹⁹ So in this study, photooxidation of p-xylene is performed using UV-irradiation of p-xylene/CH₃ONO/NO/air mixtures in our home-made smog chamber, and ATOFMS was employed to detect the particles in different reaction times. Aromatic aldehyde, saturated dicarbonyls, di-unsaturated 1,6-dicarbonyls, hydroxyl dicarbonyls, organic acid, are major products components in the SOA after 2 hours of photooxidation. After aging for more than 8 hours, about 10% of the particle mass consists of oligomers with a molecular mass up to 600 daltons. The possible reac-

tion mechanisms leading to these products are also proposed.

EXPERIMENTAL SECTION

Photooxidation of p-xylene is performed using UV-irradiation of p-xylene/CH₃ONO/NO/air mixtures in an 850 L sealed collapsible polyethylene smog chamber.²⁰ Its ratio of surface to volume was 5.8 m⁻¹. Around the chamber, there was equipped with 12 sets of 40-W fluorescent black lamps symmetrically that provide radiation in the 300-400 nm region. The bag and lamps were housed inside a highly reflective enclosure to enhance light distribution. Prior to the start of the experiment, the chamber was continuously flushed with purified laboratory compressed air for 40 mins. The compressed air was processed through three consecutive packed-bed scrubbers, which contain activated charcoal, silica gel and a Balston DFU[®] filter (Grade BX) respectively, to remove trace hydrocarbon compounds, moisture and particles. 2.0 μL/L p-xylene, 20.0 μL/L CH₃ONO, 2.0 μL/L NO were injected into the chamber and mixed with the pre-existing purified air. And again the chamber was filled with the purified air to 850 L full volume. Turn on four black lamps and initiate the photooxidation reaction. Hydroxyl radicals will be generated by the photolysis of methyl nitrate in air at wavelengths longer than 300 nm.²¹ The chemical reactions leading to the formation of the OH· radical are as follows:

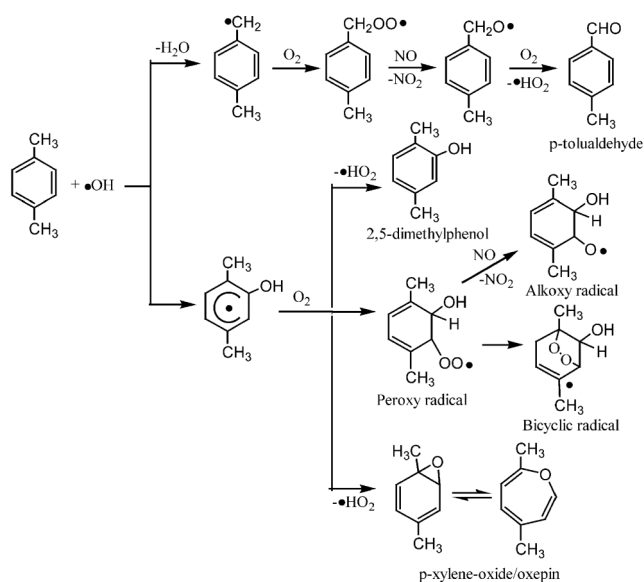
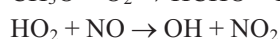
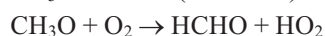


Fig. 1. Mechanistic diagram for the OH-initiated oxidation of p-xylene.

After 2 hours and 8 hours photooxidation, the SOAs produced by the photooxidation were analyzed continuously using the ATOFMS connected directly to the chamber using a Teflon line.

RESULTS AND DISCUSSION

According to the design principles on the measuring system of particle diameter, timing circuit, and laser desorption/ionization setup of ATOFMS, its time-of-flight mass spectroscopy is only obtained from those particles of secondary organic aerosol, whose diameter has been measured. The diameter of an individual particle, number distribution of SOA particle diameter, and molecular composition of an SOA particle could be measured using our

AToFMS.

Size and low-molecular-weight components of individual particle

The chemical composition and size of individual SOA particles a, b, c, and d produced from the 2 hours photooxidation of p-xylene are shown in Figs. 2a~2d. It is shown that each piece of the mass spectrum corresponds to an aerosol particle, and the diameter and chemical composition might be different from each other.

When the diameter and chemical composition of the SOA particle are detected using AToFMS, their allowable standard error on the ratio of mass to charge (m/z) is about

± 0.5 .^{22,23} Based on the typical mass spectra in Fig. 2 and a large number of other mass spectra, the chemical composition of SOA particle might be measured statistically. According to the references and possible reaction pathways of p-xylene photooxidation reaction, we can obtain the chemical composition of SOA. Table 1 lists the m/z and molecular structures of identified products from photooxidation of p-xylene, while m/z 27, 30, 38, 46, 50, 62, 66, 84, 118, 128, 134, 146, 161, 179, 183, 192, 205, and 216 represent some unidentified compounds, most of the chemical compositions of SOA particles in our results are the same as those reported in references 11-17. However, there are some differences between the current study and literature. For ex-

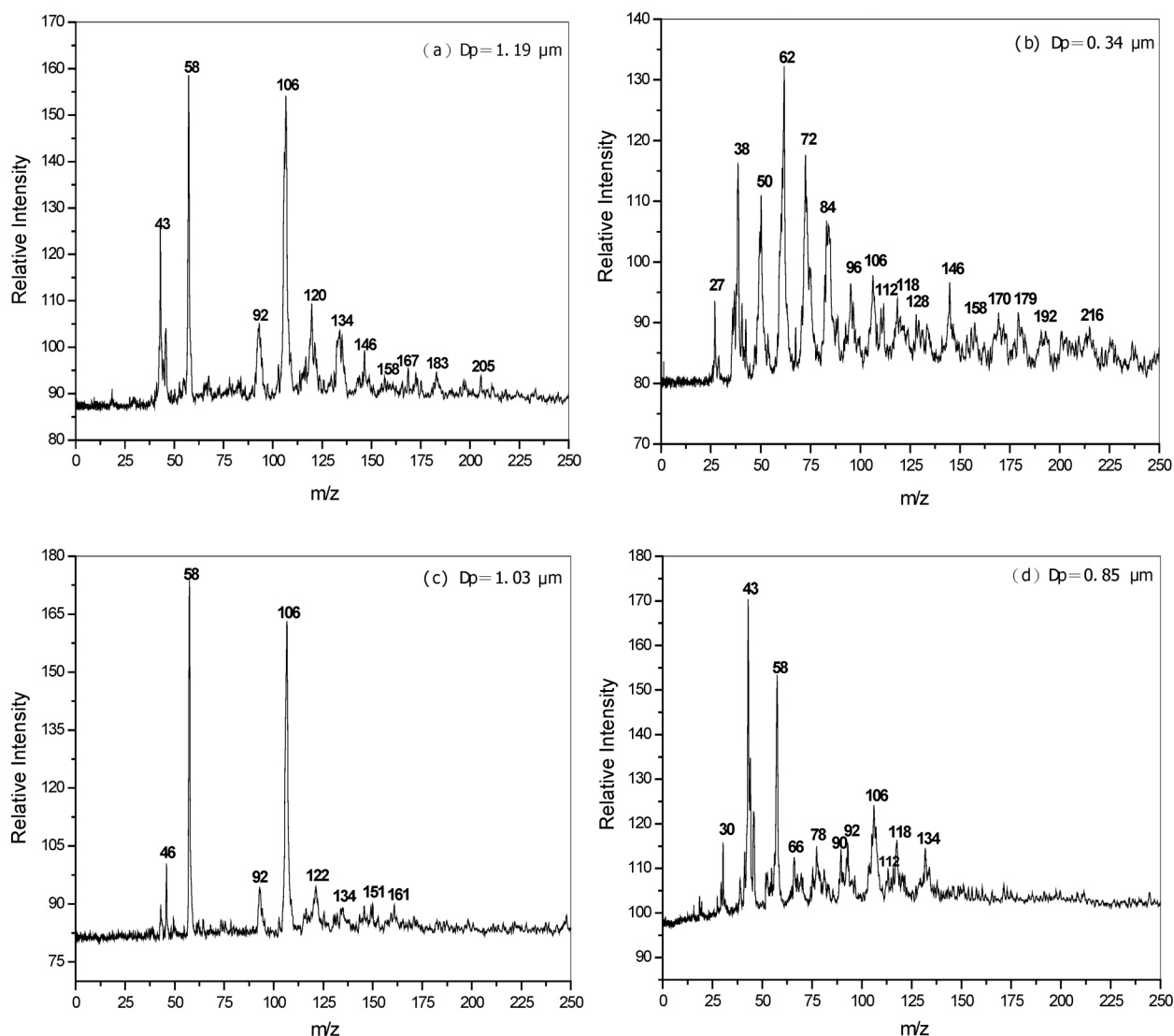
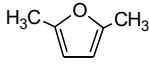
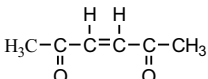
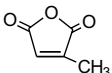
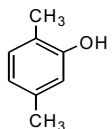
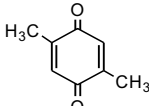
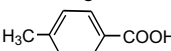
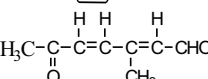
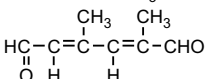
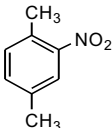
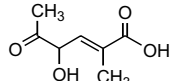
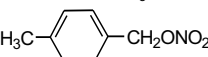
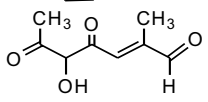


Fig. 2. Laser desorption/ionization time-of-flight mass spectra and size of 4 individual p-xylene SOA particles after 2 hours photooxidation (Aerosol diameter: (a): 1.19 μm , (b): 0.34 μm , (c): 1.03 μm , (d): 0.85 μm).

Table 1. Molecular structures of speculated products from photooxidation of p-xylene

<i>m/z</i>	Products	Structure	Ref & Comments
58	glyoxal	HCOCOH	11-17
72	methylglyoxal	CH ₃ COCOH	11-17
90	oxalic acid	HOOC-COOH	15
92	2,5-dimethylfuran		14,15
96	2-furaldehyde		13
106	p-xylene		p-xylene precursor
112	3-hexene-2,5-dione		11,14-15
	3-methyl-2,5-furandione		13,15
120	p-tolualdehyde		11-17
122	2,5-dimethylphenol		11,13-17
136	2,5-dimethyl-1,4-benzoquinone		11,13-15
	p-toluic acid		13
138	3-methyl-6-oxo-2,4-heptadieneal		16
	2,5-dimethyl-2,4-hexadienedial		16
151	2-Nitro-p-xylene		14,15
158	2-methyl-4-hydroxy-5-oxo-2-hexaenoic acid		Newly identified
167	p-methylbenzyl nitrate		17
170	2-methyl-5-hydroxy-4,6-dioxo-2-hepteneal		Newly identified

ample, 2-methyl-4-hydroxy-5-oxo-2-hexaenoic acid, 2-methyl-5-hydroxy-4,6-dioxo-2-hepteneal, and some unidentified compounds are newly found in our experiments. It is possibly due to that we detected the particles of SOA using different sample preparation and analyzing technol-

ogy.

p-Xylene photooxidation mechanisms

Possible mechanisms leading to the p-xylene-OH photooxidation products identified as SOA components are de-

pictured in Figs. 3-5. The species identified in the aerosol phase are highlighted in the mechanisms by boxes. Carbonyl products in the ring-opening route have been suggested as an important radical source and have a large impact on ozone formation in the aromatic hydrocarbon oxidation.²⁴ The bicyclic route is a major ring opening product channel for the OH-p-xylene system. Bicyclic radicals resulting from the primary peroxy radical form secondary peroxy radicals on addition of O₂ which then react with NO to form bicyclic alkoxy radicals (Fig. 3). The bicyclic alkoxy radicals can further decompose to form unsaturated dicarbonyl (2-methyl-butenedial and 3-hexene-2,5-dione in Fig. 3) and corresponding α -hydroxy radicals. Subsequent abstraction of α -hydroxy radicals by O₂ results in the formation of glyoxal and methylglyoxal (Fig. 3) respectively. 2-Methyl-butenedial has been postulated to lose a hydrogen atom from the carbonyl group via OH radical attack, with subsequent O₂ addition and rearrangement to form 3-methyl-2,5-furandione.¹³ The details of this mechanism are outlined in Fig. 3.

In polluted areas the concentration of both aromatics and nitrogen oxides is significant. Moreover, the ROO+NO reaction is generally fast.²⁵ With sufficiently high NO_x concentration, O abstraction by NO from the primary peroxy radicals leading to form alkoxy radical can play a role. As

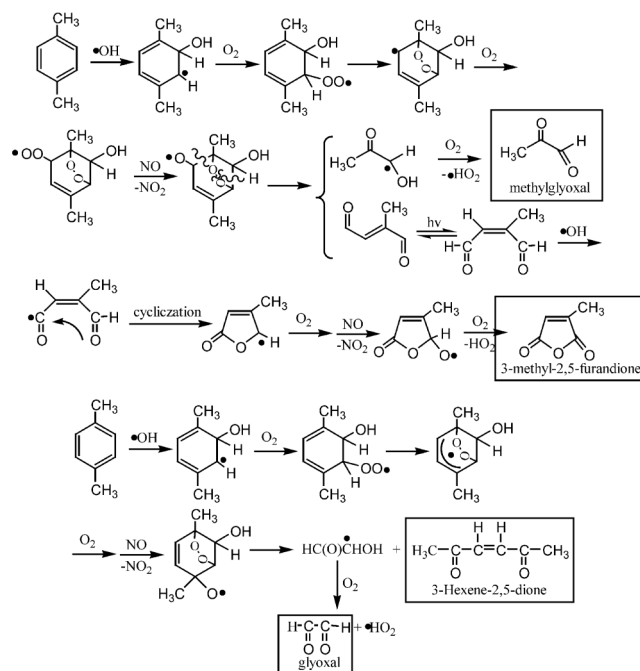


Fig. 3. Mechanistic diagram of the bicyclic pathway from OH-initiated oxidation of p-xylene.

shown in Fig. 4, the outcome of the subsequent ring opening via β -fragmentation can ultimately be the production of unsaturated dicarbonyls, 2,5-dimethyl-2,4-hexadienedial and 3-methyl-6-oxo-2,4-heptadieneal.

The atmospheric chemistry of toluene oxide/oxepin has been studied by Klotz et al., and aromatic-oxide/oxepin is fairly reactive toward OH radicals, with a reaction rate of $2 \times 10^{-10} \text{ cm}^3 \text{ molecule}^{-1} \text{ s}^{-1}$ for toluene-oxide with OH radicals.²⁶ As shown in Fig. 5, addition of OH to C6 position of p-xylene-oxide with successive ring cleavage and then H-abstraction by O₂ leads to the formation of unsaturated 1,6-dicarbonyls, 2-methyl-6-oxo-2,4-heptadieneal. In the presence of OH, O₂ and NO, 2-methyl-6-oxo-2,4-heptadieneal can further react to form 2-methyl-5-hydroxy-4,6-dioxo-2-hepteneal.

Addition of OH to C4 position of p-xylene-oxide with successive ring cleavage and then H-abstraction by O₂ leads to the formation of 1,4-dimethyl-2,3-benzoquinones. 1,4-dimethyl-2,3-benzoquinones can be attacked by OH radicals, O₂, and NO, with successive ring cleavage and then O abstraction by HO₂ leads to the formation of 2-methyl-4-hydroxy-5-oxo-2-hexanoic acid. The details of this mechanism are demonstrated in Fig. 5.

Oligomer components of individual particle

Most of the mass spectra of the p-xylene SOA after 2 hours and 8 hours photooxidation appear to have similar patterns as shown in Fig. 2, implying that the chemical

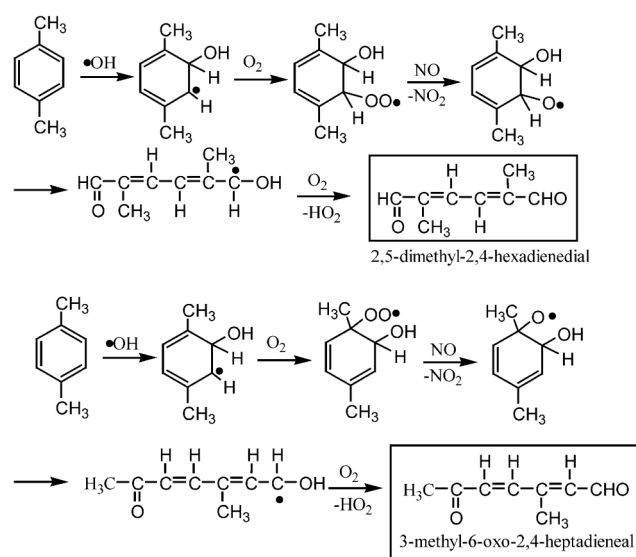


Fig. 4. Mechanistic diagram of the alkoxy pathway from OH-initiated oxidation of p-xylene.

composition of the products does not markedly change overall with the irradiation time. However, after aging for more than 8 hours, about 10% of the particle mass consists of m/z up to 600 daltons. The typical mass spectra of these kinds of particles are shown in Fig. 6. We can see that m/z 180, 252, 324, 396, 468, 540, showing the repetitive groups with $m/z = 72$, indicative of the oligomeric species.

The traditional view of SOA formation is that gas-phase oxidation of the parent hydrocarbons leads to the multifunctional, low volatility products that partition themselves between the gas and aerosol phases.²⁷ It has been assumed that, once in the aerosol phase, the oxidation products did not react further and that the amount of SOA formed depended entirely on the gas-particle partitioning. However, recent discoveries show that once the gas-phase polar oxidation products (e.g. aldehydes and ketones) condense

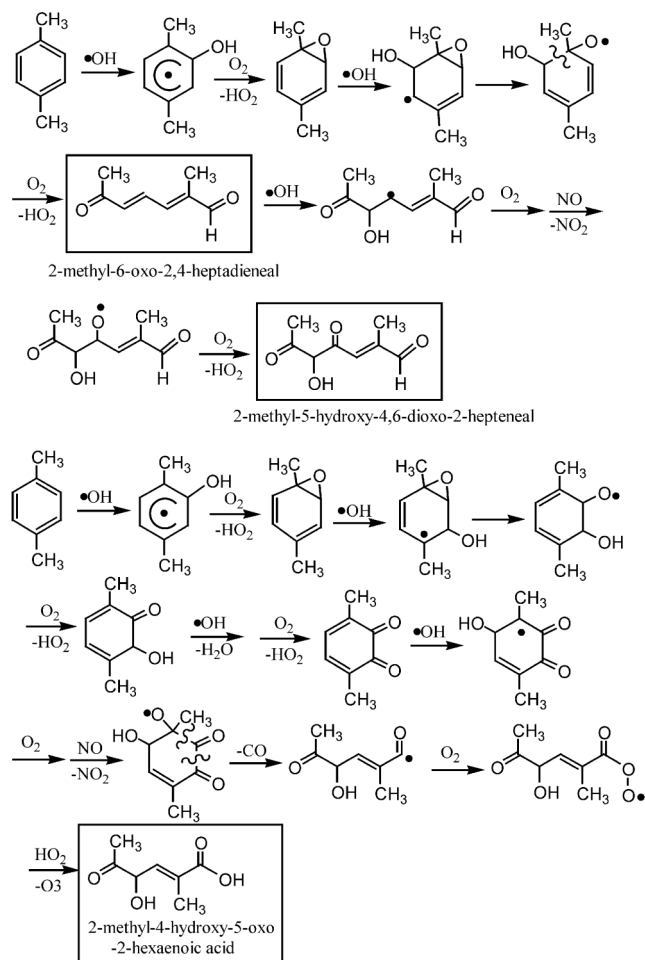


Fig. 5. Mechanistic diagram of the p-xylene-oxide pathway from OH-initiated oxidation of p-xylene.

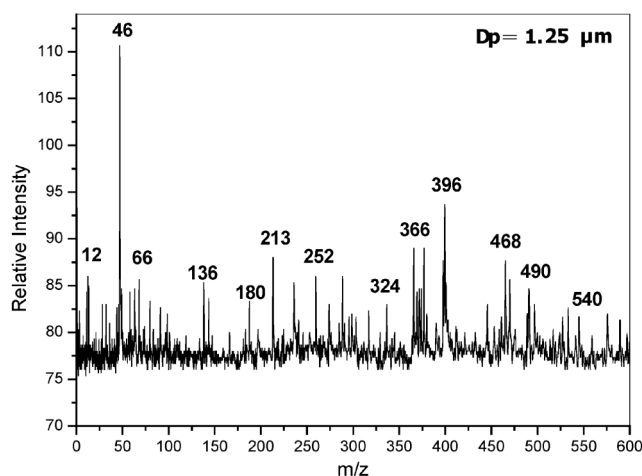


Fig. 6. Laser desorption/ionization time-of-flight mass spectra of individual p-xylene SOA particles after 8 hours photooxidation (Aerosol diameter: 1.25 μm).

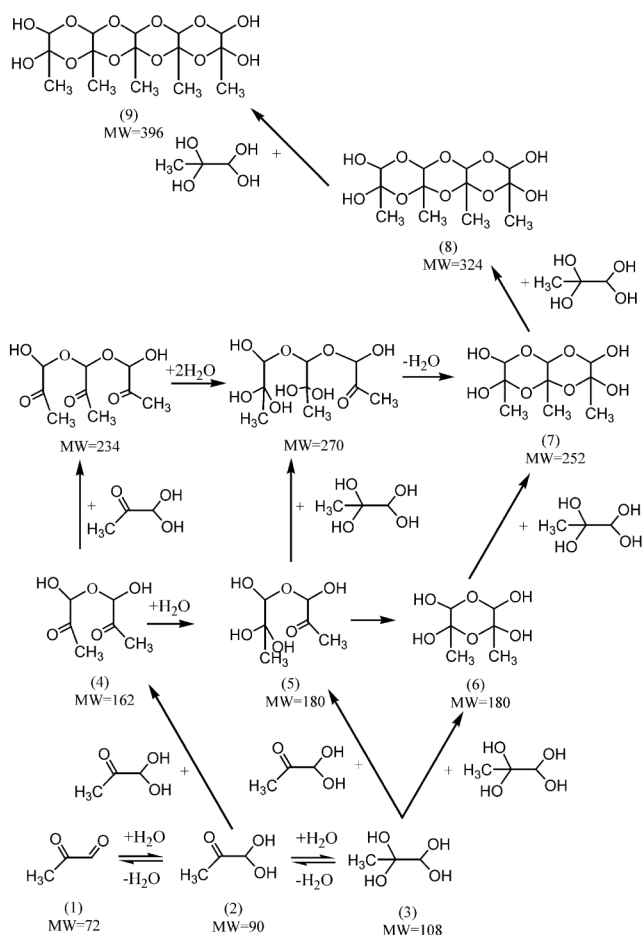


Fig. 7. Proposed reaction mechanisms leading to the formation of oligomers.

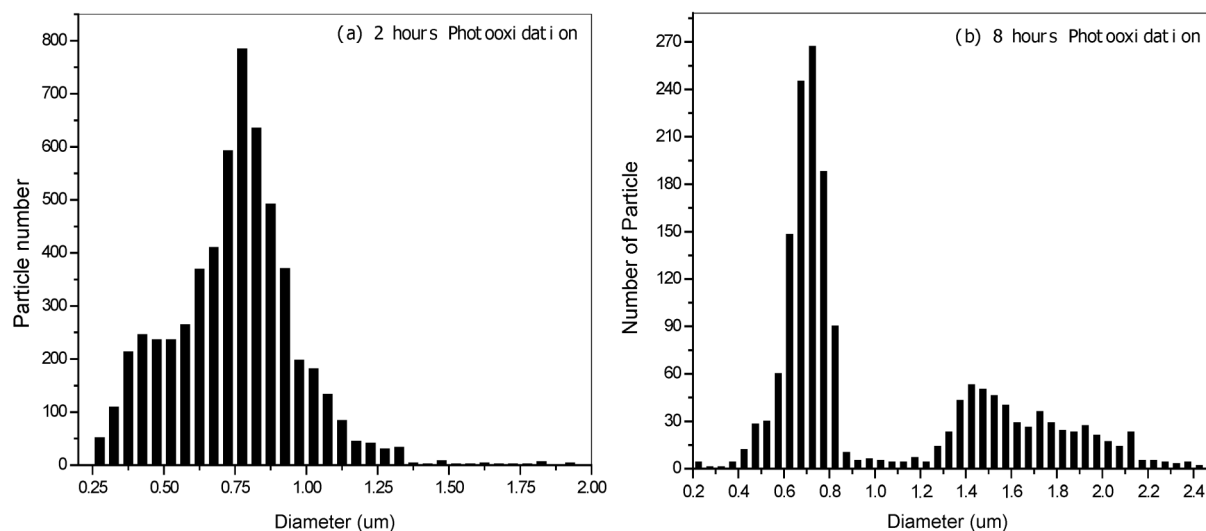


Fig. 8. Diameter distribution of p-xylene SOA particles after 2 hours and 8 hours photooxidation detected by ATOFMS (Aerosol diameter: (a): 2 hours photooxidation, (b): 8 hours photooxidation).

into the aerosol, particle phase reactions may take place.²⁸ Recently studies have demonstrated that acid-catalyzed heterogeneous reactions can occur. Possible reaction mechanisms for acid-catalyzed aldehyde reactions include hydration, polymerization, hemiacetal/acetal formation, and aldol condensation.²⁹ And the polymerization can lead to the formation of oligomers in the aerosol phase.

Carbonyls and acids have been measured in the gas and particle phase products of the p-xylene photooxidation experiments. Methylglyoxal, a C₃-dicarbonyl, was found to be one of the most abundant gas-phase photooxidation products of p-xylene.^{11,12,14-17} And the acid products, such as p-toluic acid and oxalic acid catalyze the heterogeneous reaction of methylglyoxal on secondary organic aerosols. The net result is leading to the formation of oligomers in particles. As shown in Fig. 7, initial dissolution and hydration of methylglyoxal (1) result in the diol formation (2), and further hydration produces a tetrol (3). And self-reactions and cross-reaction between diols and/or tetrols produce oligomers as shown in Fig. 7. Evidence has been provided for the formation of the dimers (4, 5, and 6) in aqueous methylglyoxal solution.³⁰ The produced dimers (4, 5, and 6) further engage in reaction with diols or tetrols to yield higher oligomers (7, 8, and 9).

Size distribution

When the chemical composition of the aerosol particles were analyzed, the number distribution of secondary

organic aerosol particles were also discussed at the same time. The number distribution of SOA particles, produced from 2 hours and 8 hours photooxidation of p-xylene, as a function of particle size is shown in Fig. 8. Under the experimental conditions mentioned above, the longer the reaction time was, the larger the particle diameter was. This is because the fine particles of matter became larger through a self-nucleation or condense on the pre-existing aerosol process; also the consequence of acid-catalyzed heterogeneous reactions and oligomer formation is that species that partition between the gas and aerosol phases are converted to larger compounds of extremely low volatility, thereby locking gas carbonyl products into the aerosol phase and increasing the diameter of the particles. And aerosol created by p-xylene is predominant in the form of fine particles, which have diameters less than 2.5 μm (i.e. PM_{2.5}), researchers have shown that this fine particulate matter is more easily deposited in the lungs of human beings, and does great harm to the health.³¹

ACKNOWLEDGMENT

This work is supported by the National Natural Science Foundation of China (20477043) and the Knowledge Innovation Foundation of Chinese Academy of Sciences (KJCX2-SW-H08). The authors express our gratitude to the referees for their value comments.

Received September 6, 2007.

REFERENCES

1. Black, F. M.; High, L. E.; Lang, J. M. *J. Air Pollut. Control Assoc.* **1980**, *30*, 1216.
2. Legett, S. *Atmos. Environ.* **1996**, *30*, 215.
3. Sye, W.-F.; Hwang, S.-S. *J. Chin Chem. Soc.* **1989**, *36*, 235.
4. Tseng, C.-M.; Dyakov, K. A.; Huang, C.-L.; Lee, Y.-T.; Lin, S.-H.; Ni, C.-K. *J. Chin Chem. Soc.* **2006**, *53*, 33.
5. Odum, J. R.; Jungkamp, T. P. W.; Griffin, R. J.; Flagan, R. C.; Seinfeld, J. H. *Science* **1997**, *276*, 96.
6. Kalberer, M.; Paulsen, D.; Sax, M.; Steinbacher, M.; Dommen, J.; Prevot, A. S. H.; Fisseha, R.; Weingartner, E.; Frankevich, V.; Zenobi, R.; Baltensperger, U. *Science* **2004**, *303*, 1659.
7. Gross, D. S.; Gälli, M. E.; Kalberer, M.; Prevot, A. S. H.; Dommen, J.; Alfarra, M. R.; Duplissy, J.; Gaeggeler, K.; Gascho, A.; Metzger, A.; Baltensperger, U. *Anal. Chem.* **2006**, *78*, 2130.
8. Atkinson, R.; Arey, J. *Chem. Rev.* **2003**, *103*, 4605.
9. Atkinson, R. *Atmos. Environ.* **2000**, *34*, 2063.
10. Suh, I.; Zhang, R. Y.; Molina, L. T.; Molina, M. J. *J. Am. Chem. Soc.* **2003**, *124*, 12655.
11. Yu, J.; Jeffries, H. E.; Sexton, K. G. *Atmos. Environ.* **1997**, *31*, 2261.
12. Kwok, E. S. C.; Aschmann, M.; Atkinson, R.; Arey, J. *J. Chem. Soc., Faraday Trans.* **1997**, *93*, 2847.
13. Forstner, H. J. L.; Flagan, R. C.; Seinfeld, J. H. *Environ. Sci. Technol.* **1997**, *31*, 1345.
14. Smith, D. F.; McIver, C. D.; Kleindienst, T. E. *J. Atmos. Chem.* **1998**, *34*, 339.
15. Kleindienst, T. E.; Smith, D. F.; Li, W.; Edney, E. O.; Driscoll, D. J.; Speer, R. E.; Weathers, W. S. *Atmos. Environ.* **1999**, *33*, 3669.
16. Volkamer, R.; Platt, U.; Wirtz, K. *J. Phys. Chem. A* **2001**, *105*, 7865.
17. Johnson, D.; Jenkin, M. E.; Wirtz, K.; Martin-Reviejo, M. *Environ. Chem.* **2005**, *2*, 35.
18. Turpin, B. J.; Saxena, P.; Andrews, E. *Atmos. Environ.* **2000**, *34*, 2983.
19. Huang, M.-Q.; Zhang, W.-J.; Hao, L.-Q.; Wang, Z.-Y.; Zhou, L.-Z.; Gu, X.-J.; Fang, L. J. *J. Chin. Chem. Soc.* **2006**, *53*, 1149.
20. Hao, L.-Q.; Wang, Z.-Y.; Huang, M.-Q.; Fang, L.; Zhang, W.-J. *J. Environ. Sci.* **2007**, *19*, 689.
21. Atkinson, R.; Carter, W. P. L.; Winer, A. M. *J. Air Pollut. Control Assoc.* **1981**, *31*, 1090.
22. Liu, D.-Y.; Wenzel, R. J.; Prather, K. A. *J. Geophys. Res.* **2003**, *108*(D7, SOS14), 1.
23. Wenzel, R. J.; Liu, D.-Y.; Edgerton, E. S.; Prather, K. A. *J. Geophys. Res.* **2003**, *108*(D7, SOS15), 1.
24. Zhao, J.; Zhang, R.; Misawa, K.; Shibuya, K. *J. Photochem. Photobiol. A* **2005**, *176*, 199.
25. Wallington, T. J.; Dagaut, P.; Kurylo, M. J. *Chem. Rev.* **1992**, *92*, 667.
26. Klotz, B.; Barnes, I.; Golding, B. T.; Becker, K. H. *Phys. Chem. Chem. Phys.* **2000**, *2*, 227.
27. Seinfeld, J. H.; Pankow, J. F. *Annu. Rev. Phys. Chem.* **2003**, *54*, 121.
28. Jang, M.; Czoschke, N. M.; Lee, S.; Kamens, R. M. *Science* **2002**, *298*, 814.
29. Jang, M.; Czoschke, N. M.; Northcross, A. L. *Chem. Phys. Chem.* **2004**, *5*, 1646.
30. Nemet, I.; Drazen, V. T.; Varga-Defterdarovic, L. *Bioorg. Chem.* **2004**, *32*, 560.
31. Schwartz, J.; Dockery, D. W.; Neas, L. M. *J. Air Waste Manag. Assoc.* **1996**, *46*, 927.